A square lattice photonic crystal fiber based surface plasmon resonance sensor with high sensitivity

Md. Abdullah Al Mamun[*], Md. Asiful Islam[*], and M. Shah Alam[*†], *Senior Member, IEEE*

[*] Dept. of Electrical and Electronic Engineering
Bangladesh University of Engineering and Technology (BUET)
Dhaka-1000, Bangladesh.

[†] Dept. of EEE, Northern University Bangladesh (on leave from BUET)
Email: shalam@eee.buet.ac.bd

***Abstract*—A surface plasmon resonance (SPR) sensor design based on four-core square lattice photonic crystal fiber (SL-PCF) has been proposed in this work. The fundamental coupling properties between the core guided light and surface plasmon polaritons are investigated here by using the finite element method (FEM). It is found that the phase matching phenomenon plays an important role in mode coupling. Through optimization of the design and numerical investigations, it is found that the use of SL-PCF with four cores yields high average sensitivity of 7432 nm/RIU in the sensing range of 1.43 to 1.50. Our study suggests that the use of SL-PCF with four cores is a promising possibility for surface plasmon resonance sensor design.**

***Keywords*—Finite element method, photonic crystal fiber, surface plasmon resonance sensor.**

I. INTRODUCTION

The surface plasmon resonance (SPR) sensors are implemented in the Kretschmann-Raether prism geometry [1], where light is passed through glass prism, which undergoes total internal reflection (TIR) from a thin metal (Au, Ag) layer deposited on the prism facet. The prism allows resonant phase matching between an incident electromagnetic wave and high loss plasmonic wave. From the requirement of miniaturization, high degree of integration and remote sensing, prism is being replaced by optical fiber. Photonic crystal fibers (PCFs), also named as micro-structured optical fibers, represent a very diverse, tunable and intriguing typology of optical fibers suitable for sensing applications such as measurement of strain, refractive index, pressure, temperature, magnetic field etc [2]. PCF-based sensors are known for their high sensitivity, small size, robustness, flexibility and ability for remote sensing [3]. Optical fiber sensors based on PCF and SPR have received considerable attention especially in the context of label-free fiber-optic biosensing in recent years [4]-[7]. Surface plasmons, which propagate in the metal-dielectric interface, are extremely sensitive to the variations of refractive index of the dielectric [8]. Implementing a SPR sensor warrants equating the effective refractive index of the plasmonic mode and core-guided fundamental mode in a particular wavelength named as resonant wavelength [9]. In the resonant wavelength, core guided fundamental mode suffers the highest loss and demonstrates loss peak due to its coupling with the plasmonic mode. Compact fiber optic SPR sensor can be constructed by passing the analyte (dielectric material to be detected) through the metal coated channel. Light entering the optical fiber, will transmit, after coupling with the plasmonic wave which is excited in the metal-analyte interface. The refractive index of the analyte can then be retrieved either by obtaining the transmission spectrum or by monitoring the transmitted power at certain wavelength [10].

Excitation of surface plasmon resonance for refractive index sensing in microstructured optical fiber with coated metal analyte channel, have actively been studied using numerical methods [1], [9]. But, in most cases the designs are based on PCFs with regular hexagonal array of air holes [11]-[13]. In this work, we have proposed a design based on square lattice PCF, which is simpler than other structural geometries.

As the real part of the plasmon refractive index depends strongly on the value of the analyte refractive index, the resonant wavelength of phase matching between the core-guided fundamental mode and plasmonic mode will also be sensitive to the changes of analyte refractive index. So with the change of the analyte refractive index, the resonant wavelength vis-à-vis the loss peak will also shift. When a new dielectric material with a different refractive index will be present in the analyte channel, it will shift the loss peak. From the amount of shift in the position of the loss peak, one can, in principle, extract the value of changes in the analyte refractive index. This transduction mechanism is commonly used for the detection of the analyte bulk refractive index changes. By implementing and optimizing the design criteria, if we can achieve greater shift of the resonant wavelength for very small change in the analyte refractive index, we can achieve high sensitivity which is investigated in this paper.

The organization of the paper is as follows. A brief, but necessary background is given in this section. In section II, we describe the design and numerical modeling procedure. Simulation of the model is conducted for a wavelength range of 0.40 μm to 1.50 μm with the analyte refractive index in a range of 1.43 to 1.50. This simulation procedure is described in section III. Numerical results are analyzed, interpreted and outcome is deduced in section IV. A brief summary is given in section V.

II. DESIGN AND MODELING

The schematic of the square lattice multi-core holey fiber (SL-MCHF) SPR sensor with four identical cores is shown in Fig.1, where a closer look of the analyte channel and the gold

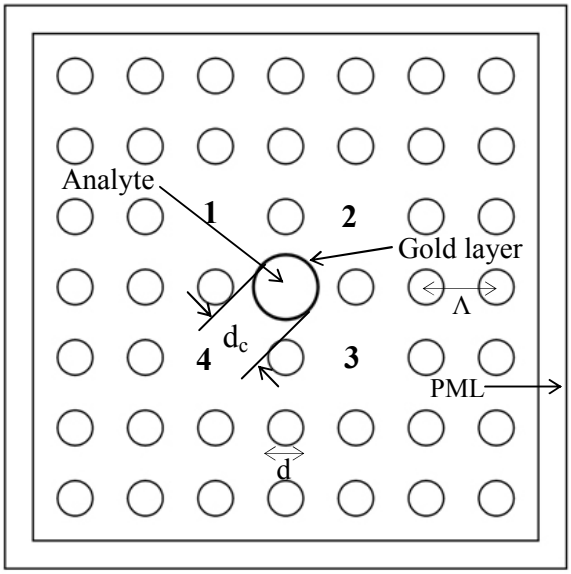

(a)

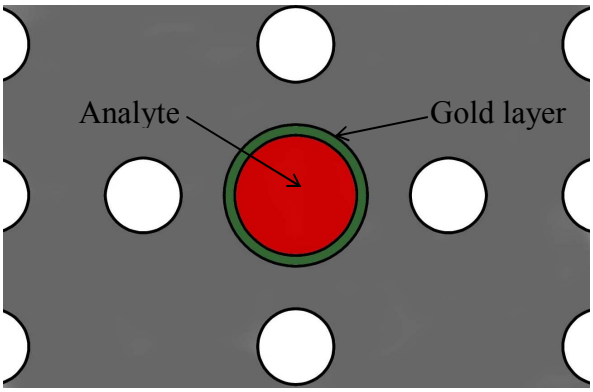

(b)

Fig. 1. (a) Schematic cross section of the proposed SPR sensor, (b) Closer look of analyte channel and gold layer.

layer is shown in Fig. 1(b). The three layers of air holes are arranged in a square lattice. The cores are formed by omitting four air holes in the first layer, which are substituted by four silica rods. The cores are marked with arabic numerals 1, 2, 3 and 4. The remaining second and third layers of air holes constitute the lower index cladding. Index guiding mechanism is used for power confinement. It is found that multiple analyte channels are used in earlier works [1], [9], [13]. It is also found that the use of a small air hole in the core center to achieve phase matching condition is not necessary, which is practiced in previous configurations [1], [9], [14]-[15]. In our design, instead of using a small air hole in the center and multiple analyte channels, only one analyte channel in the center of the cross section is used. This design can be obtained by mature stack-and-draw fabrication process [16]. The inclusion of analyte in the central area can effectively increase the overlap between the evanescent field generated out of TIR on metallic layer and the analyte. This enhancement of overlap, through this design, increases the detection sensitivity of the SPR sensor [17].

The PCF is made of silica glass with air holes running along the length where the air holes are arranged in square lattice having pitch Λ = 2μm. The diameter of the central analyte channel is d_c= 0.9Λ and the diameter of the air holes are d = 0.5Λ. The metalized micro channel is coated with gold of thickness t = 40nm. A commercially available software COMSOL Multiphysics has been used for modeling and investigating the mode characteristics. A perfectly matched layer (PML) is used in the boundary and the wavelength dependent refractive index of silica material is found using Sellmeier equation. The dielectric constant of gold is obtained from the Drude model [1], [18]. The metalized micro channel is filled with aqueous sample named as analyte, with n_a varying from 1.43 to 1.50.

III. Simulation Procedure

For a particular wavelength, the complex effective refractive index of core-guided fundamental mode and plasmonic mode is found out through post processing and visually investigating the mode characteristics. The power concentration of core-guided fundamental mode and the plasmonic mode for n_a = 1.43 at λ=1400 nm is shown in Fig. 2. Fig. 2(a) exhibits that the total power is concentrated in the core for core-guided fundamental mode while there is no power in the analyte channel. Again in Fig. 2(b), almost the total power is concentrated in the analyte channel for plasmonic mode while there is very negligible power in the core areas. In the analyte channel, in case of plasmonic mode, the highest power concentration is available in the metal-dielectric interface which gradually decays from the highest value at the metal-dielectric interface to the lowest value towards the center of the channel. The highest power concentration in metal-dielectric interface and the gradual decays of power in the analyte channel conform to the theory of formation of plasmonic wave [19].

In Fig. 3, the real part of effective refractive indices of core guided fundamental mode and plasmonic modes when n_a = 1.43 are plotted against wavelength ranging from 0.40 μm to 1.40 μm. From Fig. 3 it is evident that the real part of effective refractive index of core-guided fundamental mode and plasmonic mode intersect at wavelength of 865 nm.

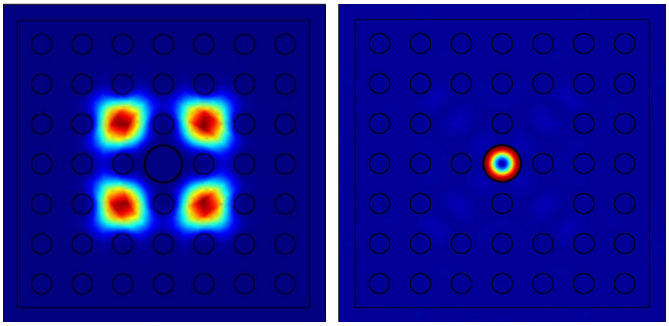

(a) n_{eff}=1.422134+3.200937e-6i

(b) n_{eff}=1.34893+0.002842i

Fig. 2. Concentration of power in, (a) core-guided fundamental mode and (b) plasmonic mode for analyte index n_a = 1.43 and λ=1400 nm.

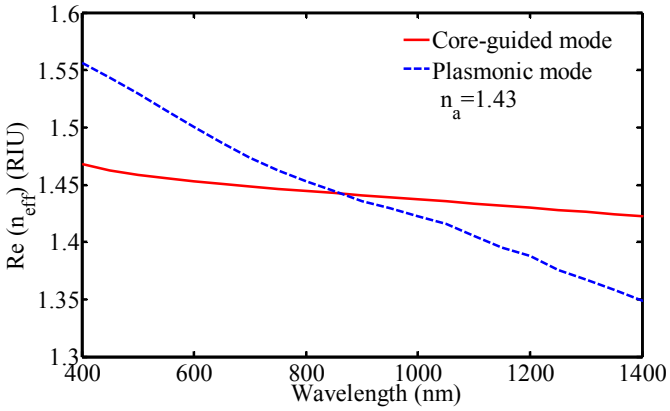

Fig. 3. Real part of effective refractive indices of core-guided fundamental mode and plasmonic mode for n_a = 1.43.

The propagation loss is calculated from the imaginary part of the complex effective refractive index of core guided fundamental mode as [1], [12]

$$\alpha = 40\pi \frac{Im(n_{eff})}{\ln(10)\lambda} \text{ dB/m} \quad (1)$$

where α is the prorogation loss expressed in dB/m, $Im(n_{eff})$ is the imaginary part of the effective refractive index of core guided fundamental mode and λ is the wavelength of operation expressed in meter. As an example, loss spectrum for n_a = 1.44 is shown in Fig. 4. From the loss spectrum, we find that there is loss peak at certain wavelength named as resonant wavelength where the coupling between fundamental mode and plasmonic mode happens. This way loss peak for each of the analyte refractive index is found out which indicates the resonant wavelength for coupling with varying analyte refractive index.

IV. Numerical Results and Analysis

Following the procedure described in section III, numerical results of all the simulation is compiled. Required analysis, comparison and interpretation is done to have a comprehensive understanding about the resonance coupling properties and also to find out the sensing performance of proposed sensor design. Interpretation is done with a view to find out the phase matching point between the core-guided fundamental mode and the plasmonic mode, and also to find the excitation of plasmonic mode in the resonant wavelength exhibited by loss peak.

A. Phase Matching and Coupling

Detection of high-index fluid can be realized by selective resonant coupling through phase matching in this four-core SL-PCF. To exhibit the phase matching and coupling properties we exemplarily consider three analyte refractive index value such as n_a = 1.43, 1.44 and 1.47. The phase matching and coupling phenomenon can be confirmed by the position of the loss peak discussed in the subsequent sub-section. The relationship of real part of effective refractive index of core-guided fundamental mode and the plasmonic mode with respect to wavelength of operation is shown in Fig. 5 for n_a = 1.43, 1.44 and 1.47. The resonance is indicated by the point of intersection which equates the real parts of the effective refractive indices of both the modes. The intersecting points in Fig. 5 are shown around the corresponding resonance wavelength for clarity. For n_a = 1.43, 1.44 and 1.47 the intersection between the core-guided fundamental mode and the plasmonic mode are found at 865 nm, 948 nm and 1160 nm, respectively.

B. Loss Calculation

The point of concern in regards to loss calculation is to find the loss peak of the core-guided fundamental mode, which is supposed to occur in the intersection points found in Fig. 5. The resonance is indicated by the core guided mode loss spectrum which presents a loss peak at resonant, i.e. highest energy transfer from the core-guided mode to plasmonic mode. The loss spectra for analyte refractive index value for n_a = 1.43, 1.44 and 1.47 with respect to wavelength is shown in Fig. 6. If we analyze the loss spectra, we find that

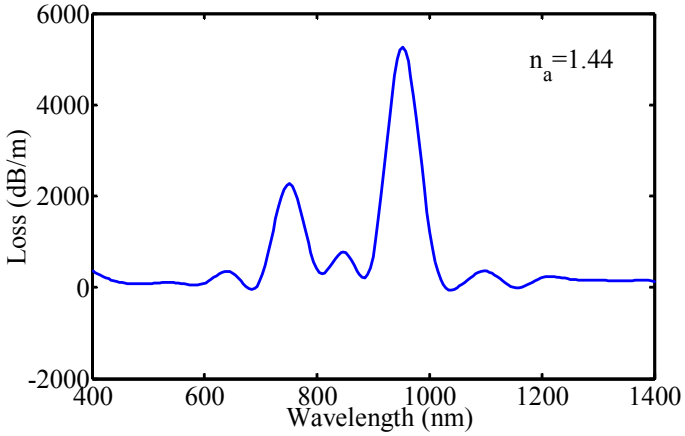

Fig. 4. Loss spectrum of core-guided fundamental mode which represents a peak at 948 nm wavelength. The spectrum is obtained for n_a = 1.44.

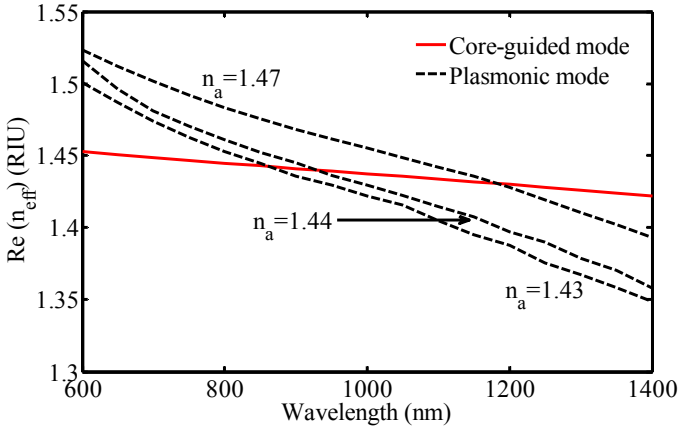

Fig. 5. Intersection of the real part of the effective refractive indices of the core-guided fundamental mode and plasmonic mode for n_a = 1.43, 1.44 and 1.47.

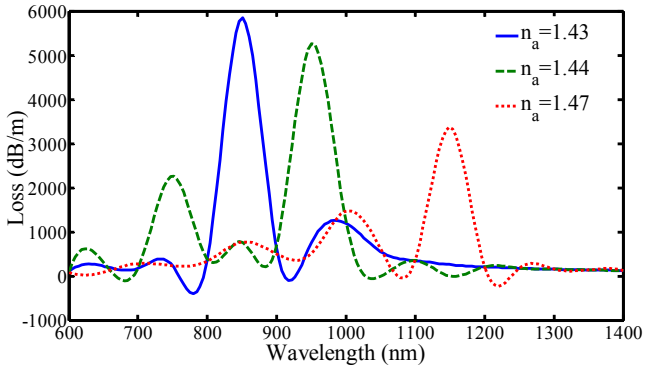

Fig. 6. The loss spectra of core-guided fundamental mode for n_a = 1.43, 1.44 and 1.47.

for different analyte refractive index value, the loss peak occurs in different wavelength. This happens because for each analyte refractive index, the plasmonic wave will have different effective refractive index, which consequently couple with the core-guided fundamental mode and create loss peak in different wavelength. The exhibits in Fig. 6 confirm the theory that the plasmonic wave depends strongly on the analyte refractive index value.

C. *Comparison of Phase Matching and Loss Calculation*

If we combine both the intersection points and the loss spectra, we can see that both happen in the same resonant wavelength which is shown in Fig. 7. For clarity both the plots are now shown in the same figure. In Fig. 7 we find that the loss peaks for analyte index 1.44 and 1.47 are found at 948 nm and 1160 nm, respectively, which are also the intersection points between core-guided fundamental mode and plasmonic modes for respective analyte refractive index.

D. *Sensing Performance*

The operation of SPR sensor is to detect any changes in the refractive index of the analyte. There are two main methods of detection. The first one is based on amplitude or phase change, computed in a single wavelength. As no spectral manipulation is required in this method, it is simple and incurs low cost. But the disadvantage of this method is lower sensitivity and small operational range. The second one is based on wavelength interrogation method in which transmission spectra are taken and compared, before and after the change in analyte refractive index. By comparing the spectra, displacement of resonant wavelength is measured and by measuring the displacement of the plasmonic peak, changes in the analyte refractive index is detected. We have used the wavelength interrogation method and measured the shift of the loss peak for changes in the analyte refractive index. For this method sensitivity is defined as [9, 12]

$$S_\lambda = \frac{d\lambda_{peak}}{dn_a} \text{ nm/RIU} \qquad (2)$$

where S_λ is the sensitivity expressed in nm/RIU, $d\lambda_{peak}$ is the

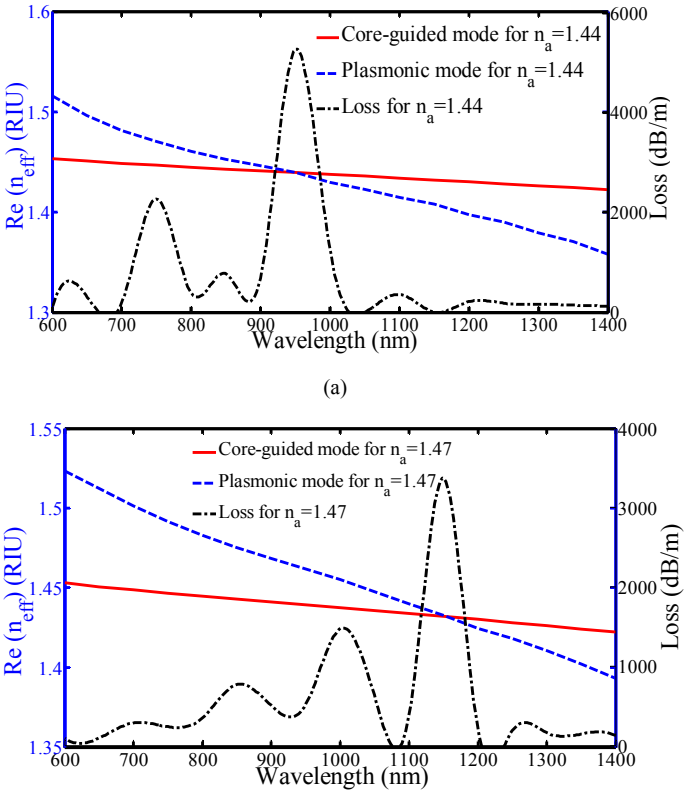

Fig. 7. Loss peak and intersection of the effective refractive indices of core-guided fundamental mode and plasmonic mode for, (a) n_a = 1.44 and (b) n_a =1.47. For clarity the phenomena are shown in the vicinity of resonant wavelength.

difference of the loss peak in nm between two loss spectra of two analyte and dn_a is the difference of the value of the analyte refractive index. By comparing between different analyte refractive index we have achieved an average sensitivity of 7432 nm/RIU.

By plotting the detected analyte refractive index and corresponding resonant wavelength, we can get an idea about the linearity of detection which is given in Fig. 8. From Fig. 8 it is evident that the proposed sensor has a high degree of linearity.

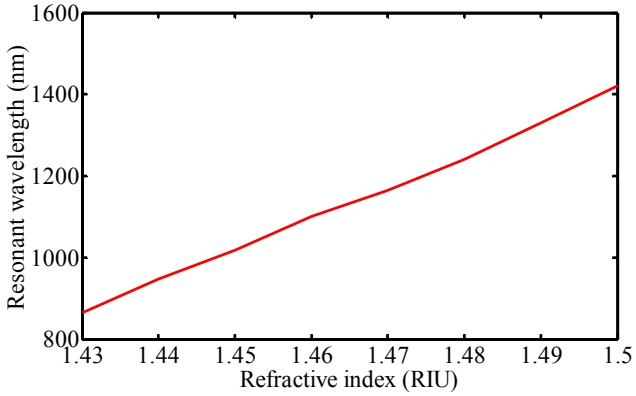

Fig. 8. Representation of detection linearity for proposed sensor design.

V. CONCLUSION

We have proposed a SPR sensor based on SL-PCF with four identical cores encircling only one analyte channel which is located in the centre of the PCF. Coupling between core-guided fundamental mode and plasmonic mode are found through phase matching. With optimized design an average sensitivity of 7432 nm/RIU is obtained in the sensing range of 1.43 to 1.50. The proposed sensor also follows almost a linear trend in terms of the shift of the resonance peak. For high sensitivity, this sensor can be used for quantitative detection of chemical and biological species. These include food quality, medical diagnostic and environmental monitoring. For high linearity and sensitivity the proposed sensor can also be used as a calibration sensor with which the analyte refractive index can be retrieved from the calibration relations.

REFERENCES

[1] A. Hassani and M. Skorobogatiy, "Design criteria for microstructured optical fiber based surface plasmon resonance sensors," *J. Opt. Soc. Am. B,* vol. 24, no. 6, pp. 1423–1429, June 2007.

[2] Luciano Mescia and Francesco Prudenzano, "Advances on Optical Fiber Sensors," *Fibers,* vol. 2, pp. 1-23, 2014.

[3] Benedetto Troia, Antonia Paolicelli, Francesco De Leonardis and Vittorio M. N. Passaro, "Photonic crystal for optical sensing: a review," in Advances in photonic crystals, Vittorio M.N. Passaro Ed., Intech, 2013, pp. 241-295.

[4] L. Rindorf, J. B. Jensen, M. Dufva, L. H. Pedersen, P. E. Høiby, and O. Bang, "Photonic crystal fiber long-period gratings for biochemical sensing," *Opt. Express,* vol. 14 no. 18, pp. 8224–8231, September 2006 .

[5] Byoungho Lee, "Review of the present status of optical fiber sensors," *Opt. Fiber Technol.,* vol. 9, pp. 57-79, 2003.

[6] L. Rindorf, and O. Bang, "Sensitivity of photonic crystal fiber grating sensors: biosensing, refractive index strain, and temperature sensing," J. *Opt. Soc. Am. B,* vol. 25, no. 3, pp. 310–324, 2008.

[7] J. R. Ott, M. Heuck, C. Agger, P. D. Rasmussen, and O. Bang, "Label-free and selective nonlinear fiber-optical biosensing," *Opt. Express,* vol. 16, no. 25, pp. 20834–20847, December 2008.

[8] Anuj K. Sharma, Rajan Jha, and B. D. Gupta, "Fiber-Optic Sensors Based on Surface Plasmon Resonance: A Comprehensive Review," *IEEE Sens. J.*, vol. 7, no. 8, pp. 1118-1129, August 2007.

[9] A. Hassani and M. Skorobogatiy, "Design of the microstructured optical fiber-based surface plasmon resonanc sensors with enhanced microfluidics," *Opt. Express*, vol. 14, no. 24, pp. 11616–11621, November 2006.

[10] Markus Hautakorpi, Maija Mattinen and Hanne Ludvigsen "Surafce-plasmon-resonance sensor based on three-hole microstructured optical fiber," *Opt. Express,* vol. 16, no. 12, pp. 8427-8432, June 2008.

[11] Yong Chen and Hai ming, "Review of surface plasmon resonance and localised surface plasmon resonance sensor," *J. Photonic Sens.,* vol. 2, no. 1, pp. 37-49, 2012.

[12] Binbin Shuai, Li Xia, Yating Zhang and Deming Liu, "A multi-core holey fiber based plasmonic sensor with large detection range and high linearity," *Opt. Express*, vol. 20, no. 6, pp. 5974-5986, March 2012.

[13] Pibin Bing, Jianquan Yao, Ying Lu and Zhongyang Li, "A surface-plasmon-resonance sensor based on photonic-crystal-fiber with large size microfluidic channels," *J. Optica Applicata,* vol. 42, no. 3, pp. 493-501, 2012.

[14] Berrand Gauvreau, Alireza Hassani, Majid Fassi Fehri, Andrei Kabashin and Maksim Skorobogatiy, "Photonic bandgap fiber based surface plasmon resonance," *Opt. Express,* vol. 15, no. 18, pp. 11413-11426, September 2007.

[15] Emmanuel K. Akowuah et al., "A novel compact photonic crystal fiber based plasmon resonance biosensor for an aqueous environment," in Photonic crystals-Innovative systems, lasers and waveguides, Alessandro Massaro Ed., Intech 2012, pp. 81-96.

[16] Bongkyun Kim Tae-Hoon Kim, Long Cui and Youngjoo Chung, "Twin core photonic crystal fiber for in-line Mach-Zehnder interferometric sensing applications," *Opt. Express*, vol. 17, no. 18, pp. 15502-15507, August 2009.

[17] Bing Sun et al., "Microstructured-core photonic-crystal fiber for ultra-sensitive refractive index sensing," *Opt. Express*, vol. 19, no. 5, pp. 4091-4100, February 2011.

[18] Viktor myroshnychenko et al., "Modeling the optical response of gold nanoprticles," *Chem. Soc. Rev.,* vol. 37, pp. 1792-1805, July 2008.

[19] Sylvain Herminjard et al., "Surface plasmon resonance sensor showing enhanced sensitivity for CO_2 detection in mid-infrared range," *Opt. Express*, vol. 17, no. 1, pp. 293-303, January 2009.